
Article:
Lord, C.E. and Huang, Z. (Accepted: 2015) The Mechanical Properties and the Influence of Parameters for Metallic Closed-Cell Foam Subjected to High-Strain Rates. Advanced Materials Research , 1119. pp. 799-806. ISSN: 1022-6680

https://doi.org/10.4028/www.scientific.net/AMR.1119.799

The Mechanical Properties and the Influence of Parameters for Metallic Closed-Cell Foam Subjected to High-Strain Rates

Charles E. Lord[1,a] and Zhen Huang[2,b]

[1]University of Sheffield, Department of Mechanical Engineering, Mappin Street, Sheffield, S1 3JD, United Kingdom

[2]Wuxi Xiexing Port Machinery CO., LTD, Luzhongnan RD. Yangshan Town, Huishan District, Wuxi City, 214156, China

[a]c.lord@sheffield.ac.uk, [b]hzfred@sina.com

Keywords: porous metal foam, closed-cell foam, high-strain rate, split Hopkinson pressure bar

Abstract. As the trend for lighter more efficient structures continues, the requirement for alternative materials follows. One material that has gained attention more recently is porous metallic foam. One drawback to these materials is that there is limited pedigree and understanding of their performance. As with all materials, the use of metallic foam for structures requires knowledge of its mechanical properties; including at high-strain rates. The focus of this paper is to determine the compressive mechanical properties and the influencing parameters for AISI 4340 steel closed-cell foam under high-strain rates ($776s^{-1}$ to $3007s^{-1}$). ANSYS commercial finite element code is used to simulate a closed-cell sample under a split Hopkinson pressure bar test. In this paper the pores are considered to be spherical in shape for simplification while various parameters such as the pore size, the number of pores, the distribution of pores, and the strain rate are varied. Each of these parameters gives this material a unique response which is presented in this paper.

Introduction

The use of metallic foam, as a structural material, has generally been considered not financially suitable. However, recently this material has become more economically viable as a direct reflection of the decrease in manufacturing costs. Metallic foam benefits from the intrinsic advantages of lower density and favourable mechanical properties, such as energy absorption, when compared to the same non-porous solid material. The characterisation of metallic foam material has been an ongoing effort. The majority of the work has been aimed toward an experimental approach with focus on the static and dynamic characterisation of usually specific commercially available material. Harte et al. [1] experimented on the fatigue behaviour for several commercially available aluminium alloy foam materials. In their work they concluded that the fatigue amplitude was nearly independent of both the relative density and the mean stress. Kanahashi et al. [2] performed dynamic compressive experiments to determine the effect of the pore size for aluminium foam material. In their work they pointed out that, for the material they tested, the static and dynamic response remained nearly unchanged for different pore sizes if the relative density was constant. Yang et al. [3] studied the localised deformation in aluminium foam using split pressure Hopkinson bar (SHPB) experiments and simulations at strain rates of $92s^{-1}$ and $328s^{-1}$. They found that localised deformation occurred near the ends of the sample for up to 80% of the total deformation. Paul and Ramamurty [4] experimented on the strain rate sensitivity for closed-cell foam material. They concluded that the energy absorbed increased with the increase in strain rate. Cady et al. [5] did experiments to find the compressive properties of a commercially available closed-cell aluminium foam under various strain rates and various temperatures. They found that under lower strain rates the strength of the aluminium foam was higher. They thought the reasoning for this was potentially from the adiabatic heating of the thin sections of the material reducing the modulus of elasticity under high strain rates. They also showed that the stiffness of the material lowered with an increase in temperature.

Although there has been a large amount of work and effort in the area for experimental characterisation for metallic foam materials, the characterisation is still considered to be imperfect [6] and difficult to extract the significance and influence of the various parameters. In this paper, these various influencing parameters are evaluated and key conclusions are drawn to provide further information for closed-cell metallic foam material.

Modelling Parameters and Process

A SHPB finite element (FE) simulation was developed inside of ANSYS Workbench using the built in explicit solver and was validated using LS-DYNA explicit. The sample used was for AISI 4340 steel. All dimensions and material properties, for both the SHPB FE model and sample, were constant for each simulation. The only exclusion to this is that the sample contained various pore distributions, size of pores, and number of pores to evaluate the sensitivity of these parameters. Details of the material properties and geometric identities are given in Table 1.

Table 1: Relevant dimensions and material properties for the SHPB and sample

Property	Value	
	Incident/ Transmission Bars	Specimen
Length (L)	1200mm	6mm
Diameter (D)	21.77mm	8mm
Density (ρ)	8470kg/m^3	7830kg/m^3
Modulus of elasticity (E)	198GPa	205GPa
Poisson's ratio (v)	0.329	0.29

For these simulations, three different constitutive models were used: Johnson-Cook plasticity model, Johnson-Cook failure model, and the Shock EOS linear model. The Johnson-Cook plasticity is used to represent the strength behaviour of the material. With this model, the stress varies with the amplitude of the strain, the strain rate, and the temperature. The yield stress is defined as

$$Sy = \left[A + B{\varepsilon_p}^n \right] \left[1 + C \ln {\varepsilon_p}^* \right] \left[1 - {T_H}^m \right], \quad (1)$$

where ε_p is the effective plastic strain, ${\varepsilon_p}^*$ is the normalised effective plastic strain rate, T_H is the homologous temperature, and A, B, n, C, and m are the initial yield stress, hardening constant, hardening exponent, strain rate constant and thermal softening exponent, respectively. The expression in the first set of brackets defines the stress as related to the strain including strain hardening. The expression in the second set of brackets represents how the yield strength behaves from the strain rate while the third set of brackets represents the thermal softening. To describe the fracture of a material, the Johnson-Cook failure model is used. The strain at fracture is defined by

$$\varepsilon_f = \left[D_1 + D_2 \, exp^{D_3 \sigma^*} \right] \left[1 + D_4 \ln \dot{\varepsilon} \right] \left[1 + D_5 T \right], \quad (2)$$

where D_1-D_5 are damage constants, σ^* is the ratio of the pressure to the effective stress, $\dot{\varepsilon}$ is the dimensionless strain rate and T is the homologous temperature. According to Eq. 2, the expression in the first set of brackets is the stress dependence, the expression in the second set of brackets is the

strain rate dependence and the expression in the third set of brackets is the temperature dependence. The total damage of the material is defined as

$$D = \sum \frac{\Delta\varepsilon}{\varepsilon_f}, \tag{3}$$

with $\Delta\varepsilon$ being the equivalent plastic strain. Once $D = 1$, fracture of the material has been evoked. All of the stresses in the elements that satisfy this damage become zero and remain at zero for the specific element. The high-strain rate impacts from these simulations create stress waves (or shock waves). These shock waves change the material response. To account for their contribution, a model that describes the equation of state (EOS) is required. The model chosen for these simulations is the Shock EOS linear model which relates the shock velocity, U_s, to the particle velocity, u_p by

$$U_s = C + su_p \tag{4}$$

where C is a velocity constant and s is a compression limiting parameter. To relate the linear thermal expansion, α, the bulk speed of sound, c_o, and the specific heat, c_v, the Grüneisen parameter is introduced as

$$\Gamma = 3\alpha c_o^{\,2} c_v^{\,-1}. \tag{5}$$

The physical phenomena of a material is only as good as the models that are used to describe them. Owing to this, and the fact that these are semi-empirical models, the data used for this material (AISI 4340) was borrowed from [7-9] and is depicted in Table 2.

Table 2: Constitutive models parameters for AISI 4340 steel

Johnson-Cook strength		Johnson-Cook failure		Linear shock EOS	
Property	Value	Property	Value	Property	Value
A	792MPa	D_1	0.05	C	4569
B	510MPa	D_2	3.44	s	1.49
n	0.26	D_3	-2.12	Γ	2.17
C	0.014	D_4	0.002		
m	1.03	D_5	0.61		

The authors of this paper have only provided an introduction into these models and refer the reader to [7-9] for extended information.

The FE model was comprised of low-order hexahedron elements with a node count of 20525. Several simulations were run with changing the number of nodes to determine an adequate mesh for convergence. The convergence criteria used was based on the strain rate and the stress-strain response. The strain rates presented throughout this paper are based on the solid sample. The actual strain rates will increase, for the same impact velocity, depending on the stiffness and density of the sample as discussed by Yang et al. [3].

The process for the FE model for the SHPB simulations was that an initial velocity was applied to the striker bar which impacted the incident bar. The use of boundary conditions to constrain the

transmission bar and without the constraint were compared. There was no noticeable difference between the results therefore no boundary conditions were used for the simulations. The strain was recorded for a pair of nodes that were equal distance from the centre of the sample for the incident and transmission bars which was then used to process the stress-strain response. A typical strain response is shown in Fig. 1.

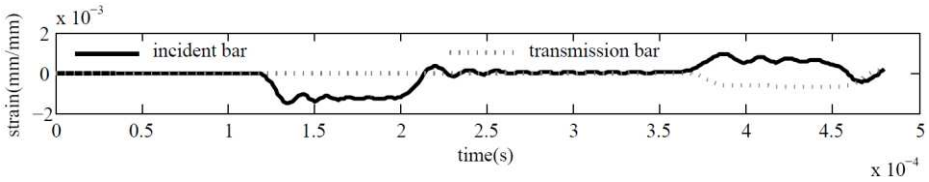

Fig. 1: Typical strain data from SHPB simulation.

One difficulty with SHPB data are the fluctuations from the stress waves inside of the sample and bars. To correct for this, a hybrid filtering technique was used. Firstly, the entire stress strain curve was filtered using a low-pass sixth-order Butterworth filter filtered above 10% of the strain step size since the strain step for each simulation varied. The data that contained fluctuations was further processed by applying a smoothing average filter with a span of 5 strain steps with a filter coefficient equal to the reciprocal of the span (0.2). These stress-strain curves were then processed to determine the yield stress and the energy absorption for each response. This paper evaluates three different parameters: pore distribution, porosity and the number of pores. In the next sections the results will be given for the influence of these various parameters.

Results and Discussion

Pore Distribution. The pore distributions considered in this paper all used a total of 8 of the same diameter of pores. Four different configurations were simulated where the pores were randomly distributed in 1 layer, 2 layers, 4 layers and all throughout the sample. The layers are defined by the coordinates through the length direction of the sample.

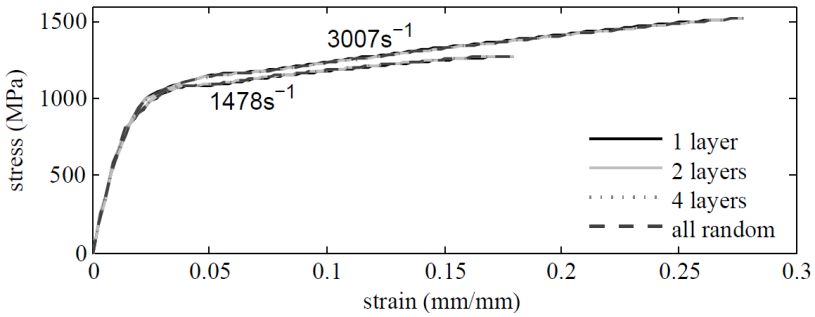

Fig. 2: Elastic-plastic engineering stress-strain curves for various planar random distributions using the same number and size of pores at different strain rates.

It is apparent that the distribution of the pores nearly unnoticeably influences the stress-strain response and that the stiffness of the sample does not change for different distributions over various strain rates.

Porosity Size. The density of metallic foam is generally around 30% of the solid material. Due to the computational demands from the required FE mesh density for such simulations, the following simulations had much higher densities (less porosity). The porosity of metal foam is related to the

size and the number of pores. To understand the behaviour of the material from changing the porosity, two groups (Group A, B) of simulations were carried out. In Group A, all simulations contained 4 pores but each simulation varied the pore diameter (0mm, 1.5mm, 2.0mm, 2.5mm). In Group B simulations, the size of the pores were held constant but the number of the pores varied between each simulation (0, 4, 8, 12).

For Groups A and B, from Fig. 3 through Fig. 6, it can be seen that the strain rate and the density both have a noticeable influence on the stress-strain response of the material. As the strain rate increases, the effective yield strength and the absorbed energy both increase which concurs with [4]. It is also that as the density decreases, the effective properties for: yield stress, modulus of elasticity and tangent modulus all decrease. Further to this, the effective yield stress related to strain rate goes from a hardening behaviour to a softening behaviour. It can also be noticed that as the density decreases, the absorbed energy related to the strain rate becomes more nonlinear for Group A. Group B however, has a much weaker nonlinearity as compared to Group A.

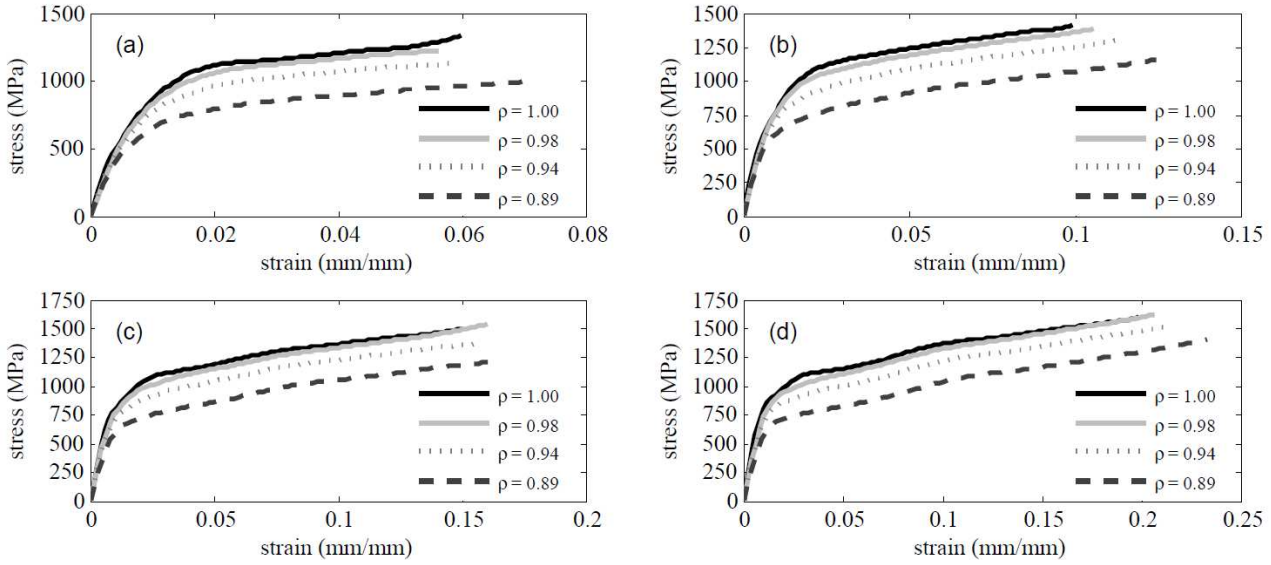

Fig. 3: Group A stress-strain response for various apparent densities using 4 pores of various diameters at different average strain rates: (a) 776s^{-1}, (b) 1478s^{-1}, (c) 2247s^{-1} and (d) 3007s^{-1}.

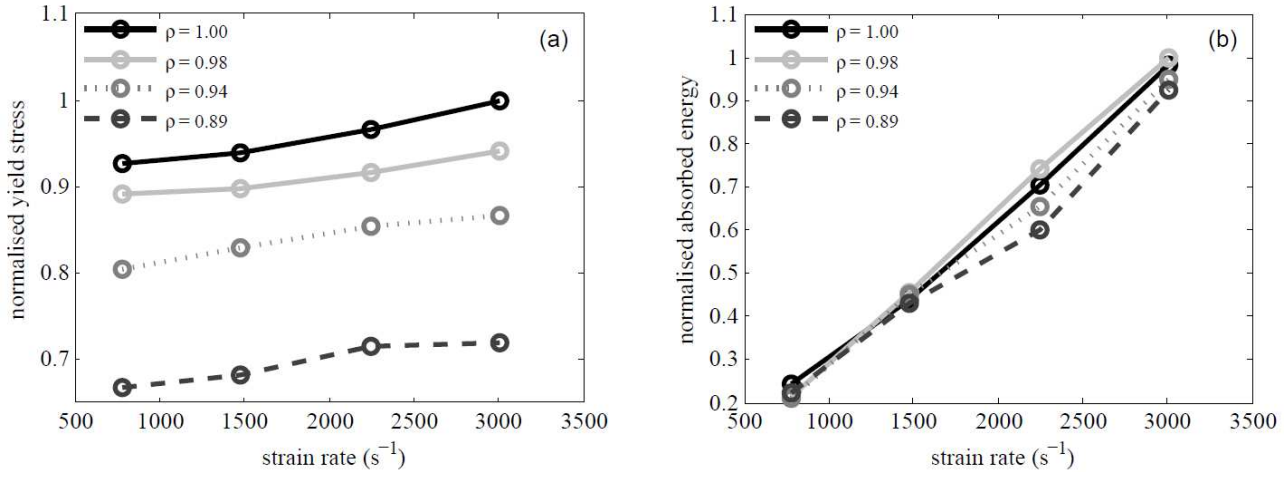

Fig. 4: Group A strain rate dependence of various densities using 4 pores with various diameters for: (a) normalised yield stress and (b) normalised energy absorption.

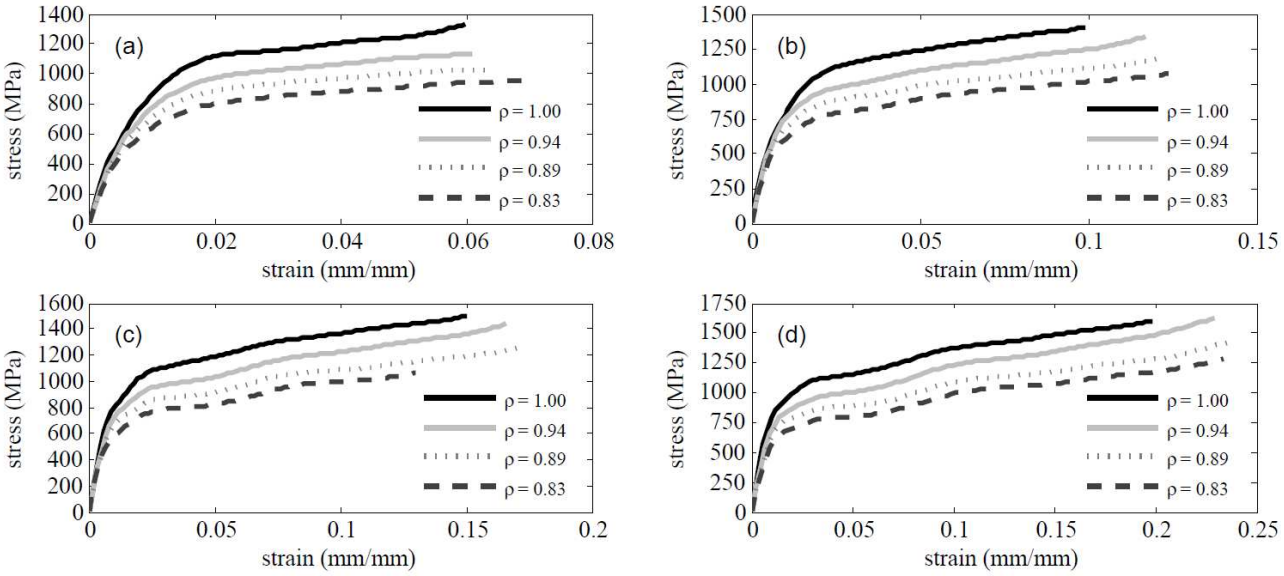

Fig. 5: Group B stress-strain response for various apparent densities using 4 pores of various diameters at different average strain rates: (a) 776s^{-1}, (b) 1478s^{-1}, (c) 2247s^{-1} and (d) 3007s^{-1}.

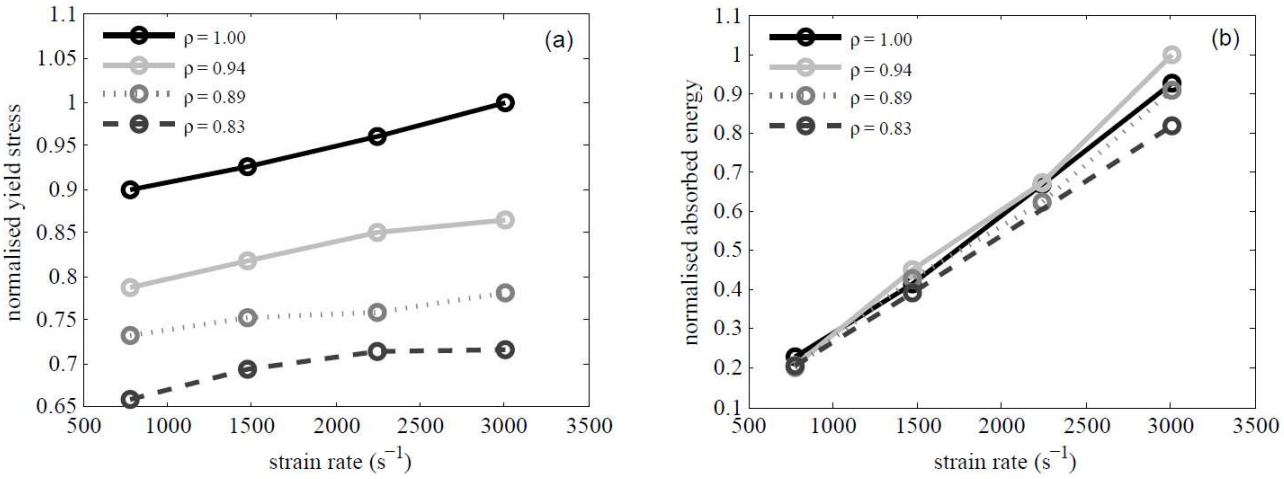

Fig. 6: Group B strain rate dependence of various densities using 4 pores with various diameters for: (a) normalised yield stress and (b) normalised energy absorption.

Number of Pores

To understand how the number of pores influences the material, simulations were run with different number of pores while the porosity was constant (ρ = 0.89). The number of pores that were included are: 0, 1, 8 and 16 denoted as ‘solid’, ‘no1’, ‘no8’ and ‘no16’, respectively.

For Fig. 7, as the number of pores increases the effective yield stress increases. This is in contrast with what was found by [2] where the response was unchanged for different pore sizes of commercially available material from experiments. Like the other simulations, as the strain rate increased, both the effective yield stress and the energy absorption increased which concurs with [4]. The effective yield stress related to strain rate goes from a hardening behaviour to a softening behaviour as the number of pores decreases but is still hardening for the ‘no16’ and ‘solid’ simulations. It is noticed that as the number of pores increases, the absorbed energy related to the strain rate becomes more nonlinear.

Unlike the other simulations, the energy absorption related to the strain rate has a softening behaviour at higher strain rates. It is also noticed that as the strain rate increases, the difference between the solid peak strain and the metal foam peak strain becomes less. This is because the pores for the higher strain rates are compressed and become in contact with one another effectively producing a solid material. This is further illustrated in Fig. 8 by the absorbed energy at lower strain rates (below 3007s-1) where the solid sample absorbs significantly less energy than the porous metal samples. This is important for when designing structures that use metal foam material to avoid total collapse of the pores to gain the optimal absorbed energy.

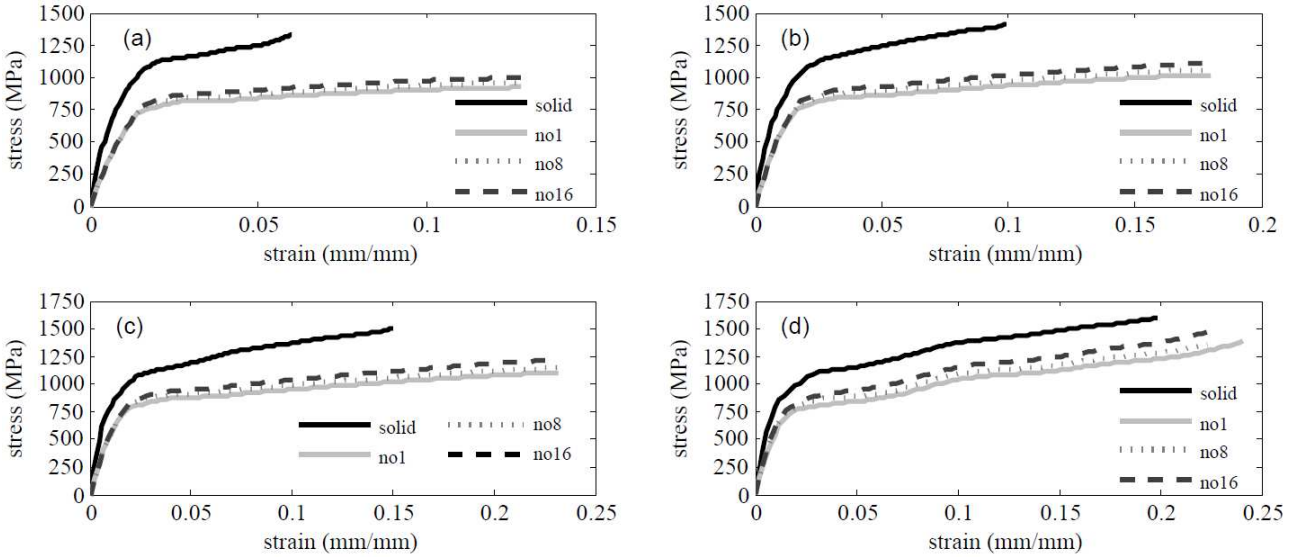

Fig. 7: Stress-strain curves for various number of pores with constant apparent density (ρ = 0.89) for different average strain rates: (a) 776s^{-1}, (b) 1478s^{-1}, (c) 2247s^{-1} and (d) 3007s^{-1}.

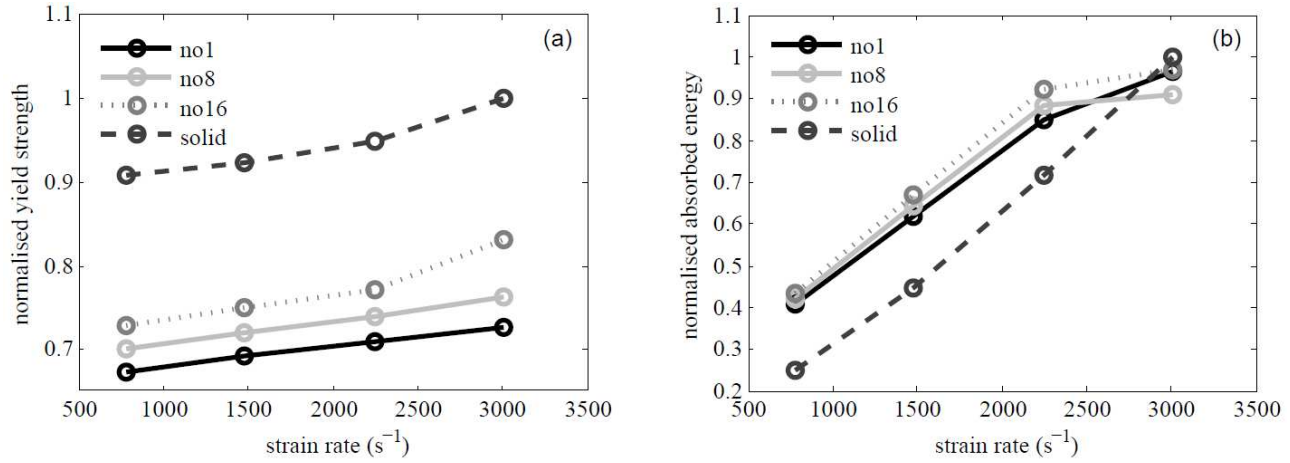

Fig. 8: Strain rate response for various number of pores: (a) normalised yield stress and (b) normalised energy absorption.

Conclusion

In this paper, simulations were presented for the influence of various parameters for closed-cell metallic foam on the material response for stress-strain and energy absorption from various strain rates. It has been shown that the distribution of the pores has little to no impact on the overall response. It is also demonstrated that the apparent density and high-strain rates not only change the stress-strain characteristics but also the level of energy absorption. Perhaps for the design of

structures that utilise metallic foam, a better way of evaluating the energy absorption is through assessing the energy absorption per density to understand the real contribution that metallic foam material is capable of producing.

References

[1] A.M. Harte, N.A. Fleck, and M.F. Ashby, Fatigue failure of an open cell and a close cell aluminium alloy foam, Acta Materiala, 47 (8), 2511-2524, 1999.

[2] H. Kanahashi, T. Mukai, T.G. Nieh, T. Aizawa, and K. Higashi., Effect of Cell Size on the Dynamic Compressive Properties of Open-Celled Aluminum Foams, Materials Transactions, 43 (10), 2548-2553, 2002.

[3] B. Yang, L. Tang, Y. Liu, Z. Liu, Z. Jiang, and D. Fang., Localized deformation in aluminium foam during middle speed Hopkinson bar impact tests, Materials Science and Engineering: A, 560, 734-743, 2013.

[4] A. Paul and U. Ramamurty., Strain rate sensitivity of a closed-cell aluminum foam, Materials Science and Engineering: A, 281 (1-2), 1-7, 2000.

[5] C.M. Cady, G.T. Gray III, C. Liu, M.L. Lovato, and T. Mukai., Compressive properties of a closed-cell aluminum foam as a function of strain rate and temperature, Materials Science and Engineering: A, 525 (1-2), 1-6, 2009.

[6] Ashby, M. F. *Metal Foams: A Design Guide*. Boston: Butterworth-Heinemann, 2000.

[7] G.R. Johnson and W.H. Cook., A constitutive model and data for metals subjected to large strains, high strain rates and high temperatures, Proc. 7th Int. Symp. on Ballistics, 541-547, Netherlands, 1983.

[8] G.R. Johnson and W.H. Cook., Fracture characteristics of three metals subjected to various strains, strain rates, temperatures and pressures, Engineering Fracture Mechanics, 21 (1), 31-48, 1985.

[9] Meyers, M.A. *Dynamic Behavior of Materials*, New York: Wiley, 1994.